

# Liver-derived Neuregulin1 $\alpha$ stimulates compensatory pancreatic $\beta$ cell hyperplasia in insulin resistance

Received: 15 April 2024

Accepted: 13 February 2025

Published online: 13 March 2025

 Check for updates

Takatomo Arai<sup>1</sup>, Eriko Hayashi<sup>1</sup>, Sumie Maeda<sup>1</sup>, Tsutomu Matsubara<sup>2</sup>, Hideki Fujii<sup>3</sup>, Koya Shinohara<sup>4</sup>, Arisu Sogabe<sup>1</sup>, Sadatomo Wainai<sup>1</sup>, Daishi Tanaka<sup>1</sup>, Yutaro Ono<sup>1</sup>, Yumika Ono<sup>1</sup>, Minami Yoshikai<sup>1</sup>, Yuriko Sorimachi<sup>5</sup>, Cindy Yuet-Yin Kok<sup>6,7</sup>, Masayuki Shimoda<sup>4</sup>, Minoru Tanaka<sup>8</sup>, Norifumi Kawada<sup>3</sup> & Nobuhito Goda<sup>1</sup>✉

Compensatory pancreatic islet hyperplasia is an adaptive response to increased systemic insulin demand, although factors mediating this response remain poorly understood. Here, we show that a liver-derived secreted protein, Neuregulin1 $\alpha$ , promotes compensatory proliferation of pancreatic  $\beta$  cells in type 2 diabetes. Liver *Neuregulin1 $\alpha$*  expression and serum Neuregulin1 $\alpha$  levels increase in male mice fed an obesity-inducing diet. Male mice lacking either *Neuregulin1* in liver or its receptor, *ErbB3*, in  $\beta$  cells deteriorate systemic glucose disposal due to impaired  $\beta$  cell expansion with reduced insulin secretion when fed the obesity-inducing diet. Mechanistically, Neuregulin1 $\alpha$  activates ERBB2/3-ERK signaling to stimulate  $\beta$  cell proliferation without altering glucose-stimulated insulin secretion potential. In patients with metabolic dysfunction-associated steatotic liver disease (MASLD) and obesity but without type 2 diabetes serum Neuregulin1 $\alpha$  levels increase, while in patient with MASLD and type 2 diabetes show markedly reduced levels of Neuregulin1 $\alpha$ . These results suggest that Neuregulin1 $\alpha$  serves as a hepatokine that can expand functional  $\beta$  cell mass in type 2 diabetes.

Compensatory pancreatic  $\beta$  cell hyperplasia is an adaptive response that maintains euglycemia in insulin-resistant states, including obesity and prediabetes, largely by stimulating the proliferation of pre-existing  $\beta$  cells and thus increasing circulating insulin levels<sup>1,2</sup>. However, this response gradually fails to meet increased systemic demands for insulin when insulin resistance and/or hyperglycemia persists, leading to exhaustion of functional  $\beta$  cells and subsequent development of overt type 2 diabetes (T2D). To prevent further disease progression and return to

a healthy state, successful restoration of functional  $\beta$  cell mass would be a promising therapeutic strategy. Therefore, elucidating molecular mechanisms underlying compensatory  $\beta$  cell hyperplasia is of great interest to many researchers in this field.

The liver is the body's central glucostat<sup>3,4</sup>: after meals, the liver consumes blood glucose by converting it to glycogen or neutral lipid. Conversely, when necessary, the liver releases glucose into the blood by either degrading hepatic glycogen or via de novo glucose synthesis from gluconeogenic substrates such as lactate and alanine. The

<sup>1</sup>Department of Life Science and Medical Bioscience, Graduate School of Advanced Science and Engineering, Waseda University, Tokyo, Japan. <sup>2</sup>Department of Anatomy and Regenerative Biology, Osaka Metropolitan University, Osaka, Japan. <sup>3</sup>Department of Hepatology, Graduate School of Medicine, Osaka Metropolitan University, Osaka, Japan. <sup>4</sup>Department of Pancreatic Islet Cell Transplantation, National Center for Global Health and Medicine, Tokyo, Japan. <sup>5</sup>Department of Stem Cell Biology, Research Institute, National Center for Global Health and Medicine, Tokyo, Japan. <sup>6</sup>Neuroscience Research Australia, Sydney, NSW, Australia. <sup>7</sup>Discipline of Medicine, Randwick Clinical Campus, University of New South Wales, Sydney, NSW, Australia. <sup>8</sup>Department of Regenerative Medicine, Research Institute, National Center for Global Health and Medicine, Tokyo, Japan. ✉e-mail: [goda@waseda.jp](mailto:goda@waseda.jp)

liver also communicates with other metabolic organs, including the pancreas by releasing liver-derived circulating factors to regulate systemic glucose metabolism<sup>5,6</sup>. Liquid chromatography-mass spectrometry analysis has identified >500 proteins secreted into the culture medium of primary murine hepatocytes, and expression of ~110 corresponding genes is known to be altered in hepatocytes from steatotic versus normal mouse liver<sup>7</sup>. These findings support the idea that liver-derived circulating proteins, known as hepatokines, serve as important regulators of systemic glucose and lipid metabolism via inter-organ communication<sup>5,6</sup>. Among these factors, however, only a few, such as serpinB1<sup>8</sup> and hepatocyte growth factor<sup>9</sup>, are known to stimulate  $\beta$  cell proliferation in vivo. Based on these findings, we hypothesized that there are liver-secreted factors that may contribute to compensatory pancreatic  $\beta$  cell hyperplasia in insulin-resistant state.

In this work, we aimed to search for hepatokines whose expression increases in proportion to compensatory hyperplasia of pancreatic islets, using microarray data collected from mice exposed to a high-fat/high-sucrose (HFHS) diet. Here, we identified type I Neuregulin1 (NRG1)  $\alpha$  as a candidate protein. Although we have previously reported an inhibitory effect of NRG1 $\alpha$  on hepatic gluconeogenesis in an autocrine and/or paracrine manner<sup>10</sup>, the endocrine role of NRG1 $\alpha$  on pancreatic  $\beta$  cells has not been addressed. Using a conditional knockout strategy, here we sought to investigate the potential of NRG1 $\alpha$  as a hepatokine that stimulates  $\beta$  cell proliferation in mice.

## Results

### Hepatic *Neuregulin1* levels correlates with pancreatic islet size

To establish a model of obesity and diabetes, we subjected normal mice to an HFHS for a 15-week period and compared them with mice fed a normal diet (Supplementary Fig. 1a). Over time, mice fed an HFHS diet exhibited obesity, liver steatosis, systemic glucose intolerance, insulin resistance, and elevated hepatic gluconeogenesis, resulting in increased serum levels of fasting blood glucose and insulin (Supplementary Fig. 1b–i), all hallmarks of diet-induced obesity with T2D and steatotic liver disease (metabolic dysfunction associated steatotic liver disease (MASLD)). Pancreatic islets in HFHS-treated mice became substantially enlarged over time, and islet hyperplasia was evident by 15 weeks (Supplementary Fig. 1j).

To search for liver-derived secreted factors underlying these phenotypes, we performed microarray analysis of liver-derived from mice fed an HFHS diet for 0, 5, 10, or 15 weeks. At 15 weeks, that analysis revealed a significant >4-fold upregulation in 118 genes and downregulation by >75% in 22 genes encoding putative secreted factors in the liver of mice fed an HFHS, although few changes (<2-fold upregulated or >one-half downregulated) were observed at 10 weeks (Fig. 1a). Among factors identified, *glycoprotein nonmetastatic melanoma protein B (Gpnmb)* was the factor most highly induced in liver of mice fed an HFHS for 15 weeks. A recent report identified GPNMB as a hepatokine acting on white adipose tissue to stimulate lipogenesis and adiposity<sup>11</sup>. Thus, we focused on the second most abundantly upregulated gene identified in the screen, *Neuregulin1* (Fig. 1a).

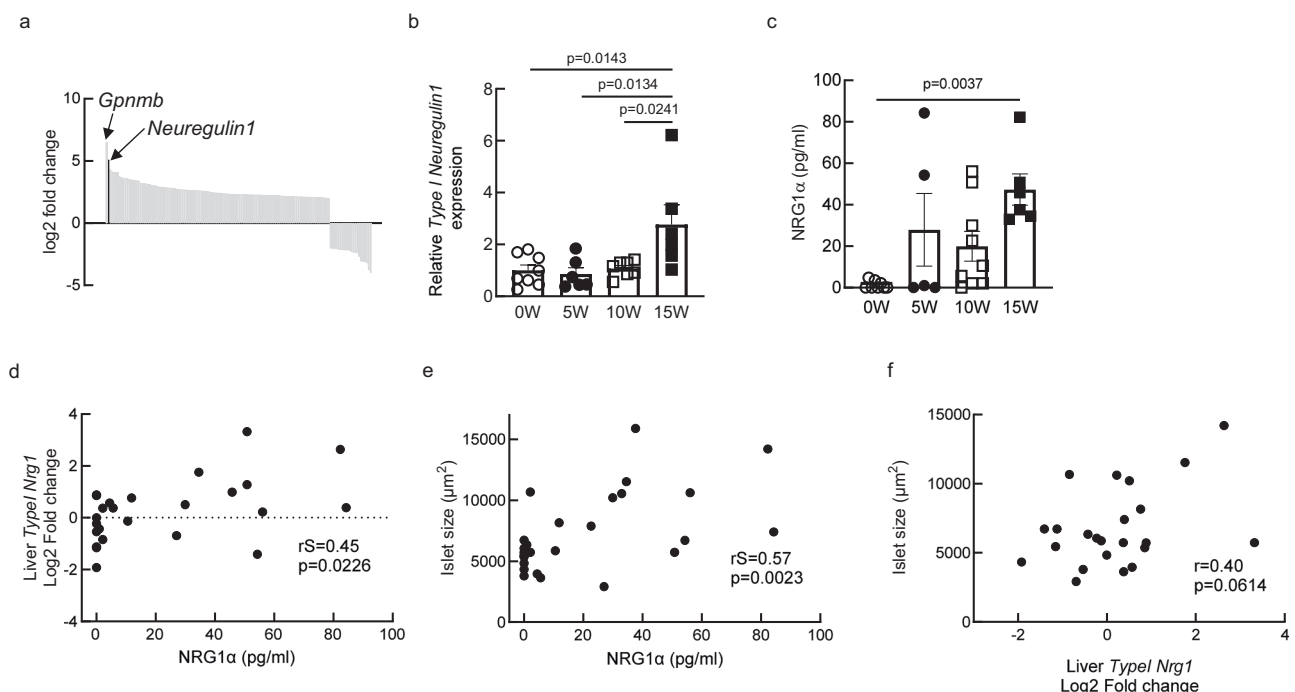


**Fig. 1 | Hepatic *Neuregulin1* expression correlates with pancreatic islet size in obese diabetic mice.** **a** Identification of *Neuregulin1* by DNA microarray analysis. Genes encoding putative hepatic factors that either increased > 4-fold (118 genes) or decreased by at least 75% (22 genes) after 15 weeks' exposure to a high-fat/high-sucrose (HFHS) diet. Overall, these genes showed little change (upregulation < 2-fold or downregulation < one-half) after 10 weeks of treatment compared to levels seen in mice before feeding. Expression levels of genes altered in mice fed an HFHS for 15 weeks were calculated as a log<sub>2</sub> ratio with reference to levels seen in mice prior to manipulation of feeding and plotted in order of increasing change in expression. The bolded black bar at left corresponds to *Neuregulin1*. **b, c** Relative quantification of hepatic type I *Neuregulin1* mRNA (**b**) and plasma Neuregulin1 $\alpha$  (NRG1 $\alpha$ ) (**c**) levels in mice fed an HFHS for the indicated times. Data represent

mean  $\pm$  SEM;  $n = 8$  (0 W), 6 (5 W), 7 (10 W) and 6 (15 W) mice per group in (**b**),  $n = 8$  (0 W), 5 (5 W), 9 (10 W) and 6 (15 W) mice per group in (**c**). **d–f** Correlation of hepatic type I *Neuregulin1* (*Nrg1*) mRNA levels (**d**) or pancreatic islet size (**e**) with plasma NRG1 $\alpha$  levels and pancreatic islet size (**f**) with type I *Nrg1* mRNA levels of mice fed an HFHS for 0–15 weeks. Pearson or Spearman's correlation analysis.  $n = 8$  (0 W), 5 (5 W), 8 (10 W) and 4 (15 W) mice per group in (**d**),  $n = 8$  (0 W), 5 (5 W), 9 (10 W) and 4 (15 W) mice per group in (**e**),  $n = 8$  (0 W), 5 (5 W), 8 (10 W) and 2 (15 W) mice per group in (**f**). A One-way ANOVA with post hoc Dunnett's multiple comparison test (**b**) and a Kruskal-Wallis test with post hoc Dunnett's multiple comparison test (**c**) was performed, and two-tailed Spearman's correlation coefficient (**d, e**) and the two-tailed Pearson correlation coefficient (**f**) were calculated.

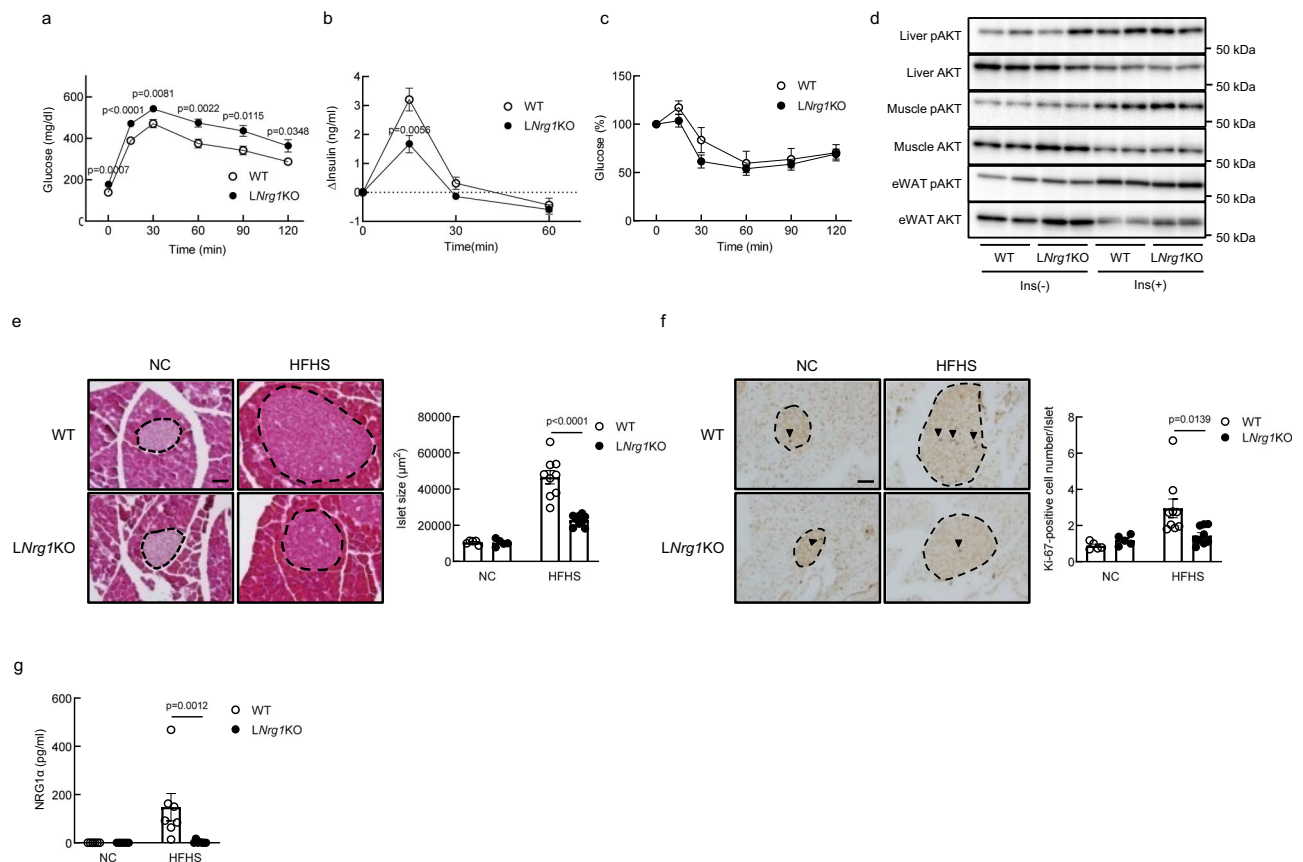


**Fig. 2 | Loss of hepatic *Neuregulin1* impairs compensatory pancreatic islet hyperplasia in obese diabetic mice. a, b** Blood glucose (a) and plasma insulin (b) levels during an oral glucose tolerance test in liver-specific *Neuregulin1* knockout (L*Nrg1* KO) and wild-type (WT) mice exposed 15 weeks to a high-fat/high-sucrose (HFHS) diet. Data represent mean  $\pm$  SEM;  $n = 12$  (blood glucose) and 11 (plasma insulin) mice per group. **c** Insulin tolerance test of L*Nrg1* KO and WT mice fed an HFHS for 15 weeks. Data represent mean  $\pm$  SEM;  $n = 6$  mice per group. No statistically significant differences were found between the two groups at any time point. **d** Immunoblotting of total and phosphorylated forms of AKT in indicated tissues of L*Nrg1* KO and WT mice fed an HFHS for 15 weeks. Tissues were harvested 15 min

after insulin (0.75 IU/kg body weight) administration. This experiment was repeated three times independently using 6 mice of each group. **e, f** Representative H&E (e) and Ki-67 (f) staining of the pancreas of L*Nrg1* KO and WT mice fed either normal chow (NC) or an HFHS for 15 weeks. Islets are enclosed by dashed lines. Black arrowheads in (f) indicate Ki-67-positive cells. Scale bar, 50  $\mu$ m. Quantification of islet area (r) and Ki-67-positive cell number (f). Data represent mean  $\pm$  SEM;  $n = 5$  (NC) and 9 (HFHS) mice per group, respectively. **g** Plasma Neuregulin1 $\alpha$  (NRG1 $\alpha$ ) levels in L*Nrg1* KO and WT mice fed either an NC or an HFHS for 15 weeks. Data represent mean  $\pm$  SEM;  $n = 6$  (NC) and 7 (HFHS) mice per group. Unpaired Student's  $t$  tests (a, b, c, e, and f) and a two-tailed Mann-Whitney U test (g) were performed.

The human *Neuregulin1* gene encodes various isoforms of Neuregulin1 protein exhibiting 6 different N-terminal types and two distinct EGF-like domains ( $\alpha$  and  $\beta$ )<sup>12</sup>; however, mouse liver predominantly expresses the type I isoform with an  $\alpha$  type EGF-like domain (designated *Neuregulin1 $\alpha$* ) (Supplementary Fig. 1k), as reported<sup>10</sup>. Quantitative PCR analysis confirmed markedly increased levels of hepatic *Neuregulin1 $\alpha$*  transcripts in mice fed an HFHS for 15 but not 10 weeks (Fig. 1b). Neuregulin1 $\alpha$  protein is cleaved to release an extracellular portion, which includes the EGF-like domain when expressed in murine hepatocytes<sup>10</sup>. Consistently, plasma levels of Neuregulin1 $\alpha$  protein also markedly increased with time in mice fed an HFHS diet (Fig. 1c), and those levels were positively correlated with levels of hepatic type I *Neuregulin1* transcripts (Fig. 1d). All other organs examined, including skeletal muscle, white adipose tissue, brain, pancreas, and small intestine, also expressed the same type of *Neuregulin1 $\alpha$* , but those levels showed minimal changes in response to an HFHS diet (Supplementary Fig. 1l, m, n). In mice fed an HFHS diet, islet size, ascertained by hematoxylin-eosin (H.E.) staining, was positively correlated with both serum Neuregulin1 $\alpha$  levels (Fig. 1e) and hepatic type I *Neuregulin1* mRNA levels (Fig. 1f), although the latter correlation was not statistically significant. Collectively, these results suggest that hepatic type I Neuregulin1 $\alpha$  could serve as a candidate hepatokine to evoke pancreatic islet hyperplasia in obese diabetic mice.

On the other hand, we also examined changes in the mRNA levels of hepatokines such as *Serp1b1* and *Hgf*, that have been reported to stimulate  $\beta$  cell proliferation and found that the mRNA levels of *Hgf*, but not *Serp1b1*, exhibited a modest increase only at 15 weeks of HFHS treatment (Supplementary Fig. 1o).

### Hepatic *Neuregulin1* loss impairs compensatory islet hyperplasia

We previously established liver-specific *Neuregulin1* knockout (L*Nrg1* KO) mice and showed that *Neuregulin1* plays a dispensable role in regulating systemic glucose metabolism in mice fed normal chow (NC)<sup>10</sup>. To test effects of an HFHS diet on these mice, we subjected L*Nrg1* KO and WT mice to an HFHS for 15 weeks to promote obesity with T2D (Supplementary Fig. 2a). During the 15-week HFHS feeding period, body weight and food intake did not differ between genotypes (Supplementary Fig. 2b, c), and liver weight/body weight and epididymal white adipose tissue weight/body weight ratios were comparable (Supplementary Fig. 2d). Interestingly, loss of hepatic *Neuregulin1* further aggravated systemic glucose disposal and promoted increased fasting blood glucose levels in mice fed an HFHS relative to WT mice (Fig. 2a). Peripheral insulin sensitivity was comparably impaired in WT and L*Nrg1* KO mice fed an HFHS diet (Fig. 2d), as was insulin-elicited AKT phosphorylation (Fig. 2d). Hepatic gluconeogenic activity, as

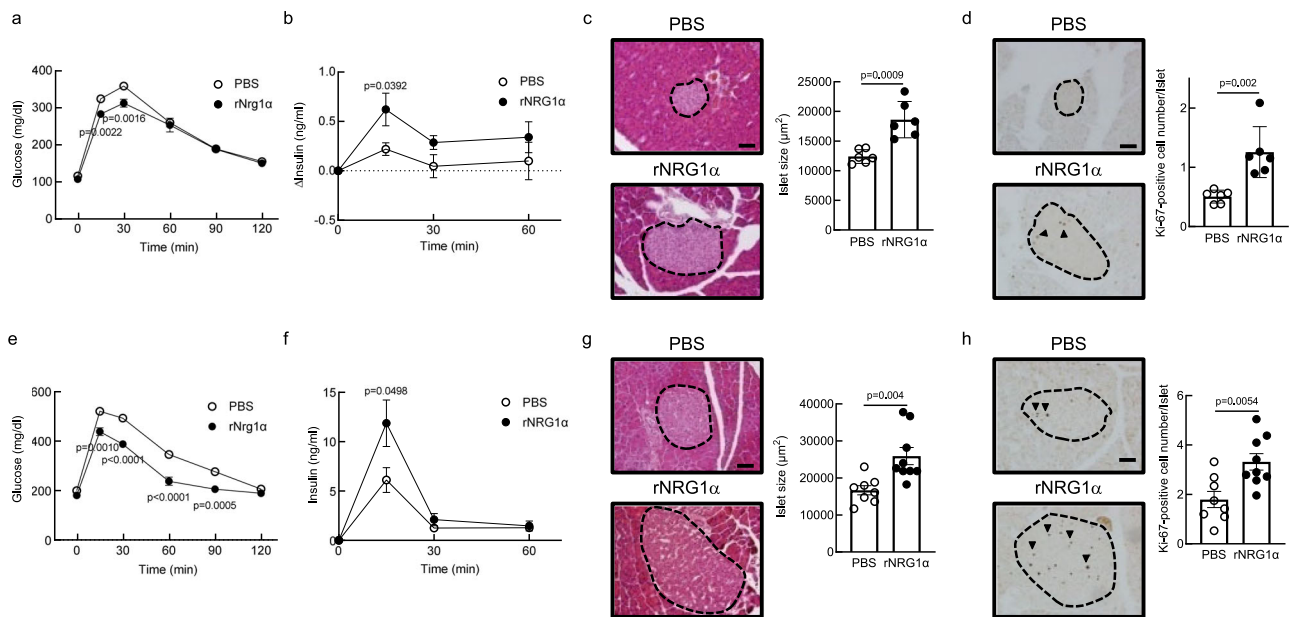


**Fig. 3 | Administration of rNRG1α enhances systemic glucose disposal with increased insulin secretion. a, b, e, f** Oral glucose tolerance test (a, e) and insulin secretion (b, f) after glucose challenge in normal (a, b) and ob/ob (e, f) mice treated for 4 weeks with recombinant protein encompassing the Neuregulin1 α type EGF-like domain (rNRG1α). Data represent mean ± SEM;  $n=10$  (PBS) and 9 (rNRG1α) mice per group (a).  $n=8$  mice per group (b).  $n=8$  (PBS) and 9 (rNRG1α) mice per group (e).  $n=10$  (PBS) and 11 (rNRG1α) mice per group (f).

assessed by pyruvate challenge, also did not differ in WT and *LNrg1KO* mice (Supplementary Fig. 2e) nor did hepatic expression levels of *Pepck* and *G6pase*, key hepatic gluconeogenic genes (Supplementary Fig. 2f). By contrast, glucose-induced insulin secretion was significantly reduced in *LNrg1KO* relative to WT mice fed an HFHS diet (Fig. 2b), accompanied by decreased compensatory islet hyperplasia (Fig. 2e) and decreased β cell proliferation, as assessed by Ki-67 staining (Fig. 2f and Supplementary Fig. 2g). Consistent with these findings, Ki-67-positive cells were observed only in β cells, but not other pancreatic endocrine cells including α cells and γ cells, of mouse islets, and the percentage of Ki-67-positive β cells was significantly reduced in *LNrg1KO* relative to WT mice fed an HFHS diet (Supplementary Fig. 2h, i). In addition, insulin/glucagon double-positive cells were not detected in our experimental conditions. *Neuregulin1* deletion in the liver also completely abolished HFHS-dependent increases in levels of serum Neuregulin1α protein (Fig. 2g), indicating that the liver is the major source of circulating Neuregulin1α in obese diabetic mice. Taken together, these results strongly suggest that hepatic Neuregulin1α is responsible for compensatory β cell expansion in obese diabetic mice.

### rNRG1α enhances systemic glucose disposal and insulin secretion

To confirm that Neuregulin1α stimulates β cell proliferation, we injected WT mice fed an NC diet with either recombinant protein encompassing the Neuregulin1 α type EGF-like domain (rNRG1α), which binds to and activates its receptors, or control PBS three times a week for a 4-week period (Supplementary Fig. 3a). As our preliminary experiments with low doses of rNRG1α (50 ng/g body weight) failed to show any impact on systemic glucose disposal after glucose challenge, we injected rNRG1α at 100 ng/g body weight in subsequent experiments to evaluate its effects. Relative to controls, rNRG1α treatment enhanced insulin secretion and slightly but significantly reduced blood glucose levels after glucose challenge (Fig. 3a, b). Islets became enlarged, and the number of Ki-67-positive

islet cells increased in rNRG1α-treated mice (Fig. 3c, d). By contrast, rNRG1α treatment did not alter peripheral insulin sensitivity (Supplementary Fig. 3b) or hepatic gluconeogenic capacity (Supplementary Fig. 3c, d). Consistently, we observed comparable responses in *leptin*-deficient obese (*ob/ob*) mice, a genetic model of type 2 diabetes (Supplementary Fig. 3a): rNRG1α treatment improved systemic glucose disposal, increased insulin secretion, resulted in larger islet size and enhanced β cell proliferation relative to outcomes seen in controls (Fig. 3e–h).

We next assessed the effects of forced hepatic expression of *Neuregulin1α* in mice fed an HFHS. To do so, we performed IP injection of adeno-associated virus serotype 8 (AAV8) harboring either *type I Nrg1α* or control *Gfp* driven by the liver-specific ApoE enhancer and hAAT promoter into mice fed an HFHS for 10 weeks followed by another 5 weeks of HFHS (Supplementary Fig. 4a). *Type I Nrg1α*-injected mice showed a ~40-fold increase in *type I Nrg1* transcript levels relative to *Gfp* controls (Supplementary Fig. 4b). Consistently, forced *type I Neuregulin1α* expression further increased Neuregulin1α protein levels in blood of mice when compared to *Gfp* controls (Supplementary Fig. 4c). Relative to controls, mice expressing *type I Neuregulin1α* showed enhanced systemic glucose disposal and increased insulin secretion (Supplementary Fig. 4d, e). Accordingly, islets in *type I Neuregulin1α*-overexpressing mice became enlarged and exhibited elevated numbers of Ki-67-positive cell numbers (Supplementary Fig. 4f, g). However, hepatic *type I Neuregulin1α* overexpression had no effects on transcripts associated with hepatic gluconeogenesis (Supplementary Fig. 4h). Collectively, these results indicate that as a hepatokine, Neuregulin1α can stimulate β cell proliferation in both basal and diabetic conditions.

### Neuregulin1α stimulates ERBB2/3-mediated ERK signaling in β cells

Neuregulin1 exerts its biological functions on target cells by binding to either ERBB (Receptor tyrosine-protein kinase erbB) 3 or ERBB4



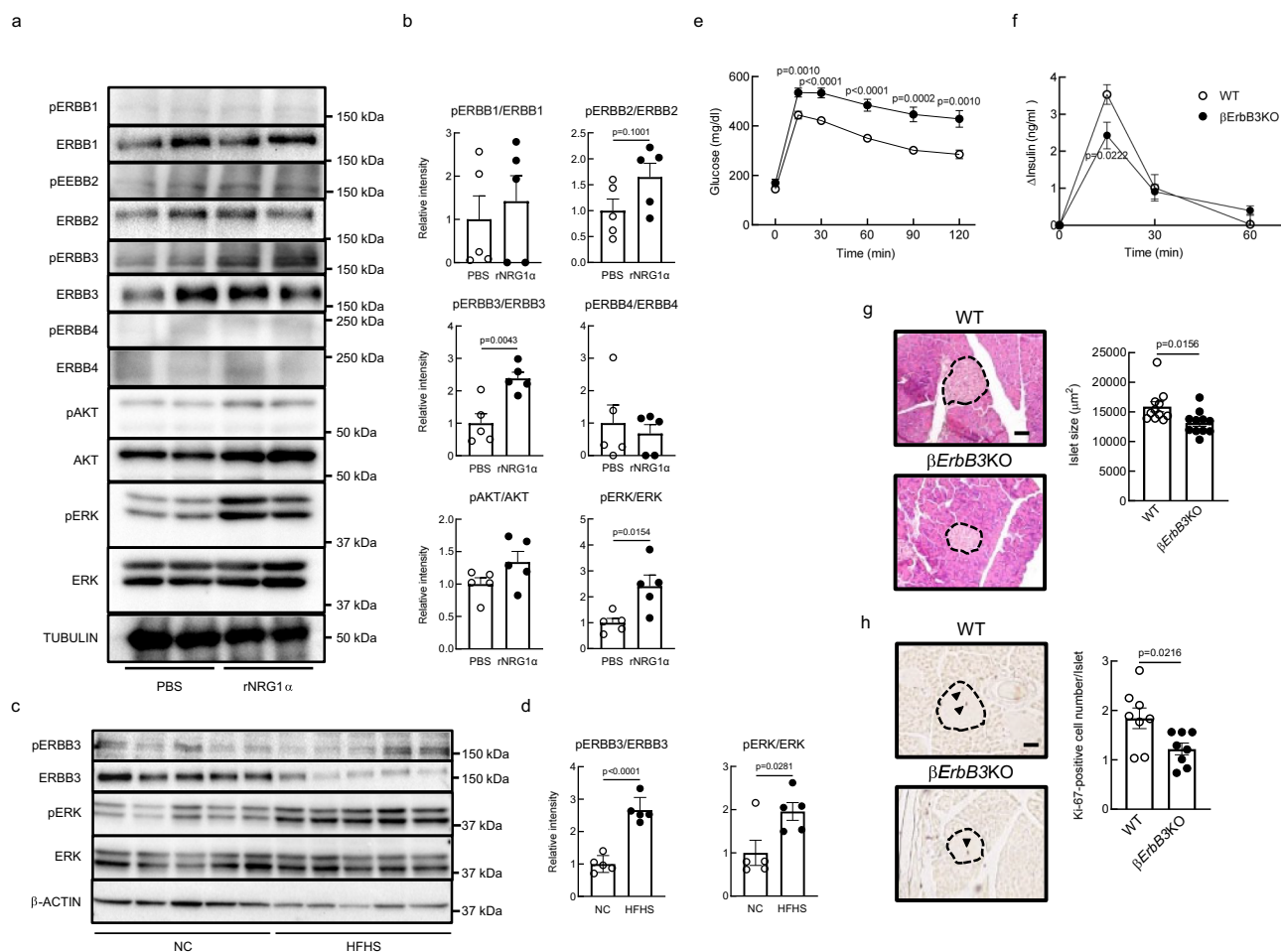


**Fig. 4 |  $\beta$  cell-specific *Erbb3* deletion impairs systemic glucose disposal and insulin secretion in obese diabetic mice. **a, b** Immunoblots (**a**) and corresponding quantification (**b**) of total and phosphorylated forms of ERBBs, AKT, and ERK in the pancreas of normal mice injected with either PBS or recombinant protein encompassing the Neuregulin1 $\alpha$  type EGF-like domain (rNRG1 $\alpha$ ). TUBULIN served as a loading control. The average value of the ratio of phosphorylated to non-phosphorylated proteins in the samples of the PBS-treated group, normalized by the expression level of TUBULIN, was set to 1. Data represent mean  $\pm$  SEM;  $n = 5$  mice per group (**b**). The samples derive from the same experiment, and blots were processed in parallel. This experiment was repeated three times independently using 5 mice of each group. **c, d** Immunoblots (**c**) and corresponding quantification (**d**) of total and phosphorylated forms of ERBB3 and ERK in the pancreas of normal mice fed a high-fat/high-sucrose (HFHS) diet for 15 weeks.  $\beta$ -ACTIN served as a**

loading control. The average value of the ratio of phosphorylated to non-phosphorylated proteins in the samples of normal mice fed a normal chow (NC), normalized by the expression level of  $\beta$ -ACTIN, was set to 1. Data represent mean  $\pm$  SEM;  $n = 5$  mice per group (**d**). **e, f** Blood glucose (**e**) and plasma insulin (**f**) levels after oral glucose challenge in  $\beta$  cell-specific *Erbb3* KO ( $\beta$ *Erbb3*KO) and WT mice fed an HFHS for 15 weeks. Data represent mean  $\pm$  SEM;  $n = 12$  (**e**) and 11 (**f**) mice per group. **g, h** Representative H&E (**g**) and Ki-67 (**h**) staining of the pancreas of HFHS-treated WT and  $\beta$ *Erbb3*KO mice. Islets were enclosed by the dashed line. Black arrowheads in (**h**) indicate Ki-67-positive cells. Scale bar, 50  $\mu\text{m}$ . Quantification of islet area (**g**) and Ki-67-positive cell number (**h**). Data represent mean  $\pm$  SEM;  $n = 11$  (**g**) and 8 (**h**) mice per group. Unpaired Student's *t* tests (**b, d, e–h**) were performed.

receptors<sup>12</sup>. To determine which receptor(s) recognizes and binds Neuregulin1 $\alpha$  in pancreatic  $\beta$  cells, we first injected rNRG1 $\alpha$  one time into normal mice and performed western blot analysis using pancreatic tissue harvested 30 min later (Supplementary Fig. 5a). We observed a marked increase in the phosphorylated form of ERBB3, but not ERBB4, in the pancreas of rNRG1 $\alpha$ -treated mice (Fig. 4a, b), suggesting selective Neuregulin1 $\alpha$  binding to the ERBB3 receptor. In consistent with these results, we also found a significant increase in phosphorylated ERBB3 levels in the pancreas by HFHS treatment, although total ERBB3 levels were reduced when exposed to an HFHS diet (Fig. 4c, d). To determine whether ERBB3 activation by ligand mediates compensatory islet hyperplasia in obese diabetic mice, we knocked out the *Erbb3* gene in pancreatic  $\beta$  cells using a tamoxifen-inducible conditional gene-knockout system<sup>13</sup> and fed mice an HFHS for 15 weeks (Supplementary Fig. 5a). As noted, this system promotes pancreas-specific deletion of *Erbb3* ( $\beta$ *Erbb3*KO) in  $\beta$  cells of adult mice, circumventing potential disruptions in pancreatic development

caused by systemic *Erbb3* deletion<sup>14</sup> (Supplementary Fig. 5b). Relative to WT controls, *Erbb3* loss in pancreatic  $\beta$  cells did not alter glucose tolerance or insulin secretion in mice fed an NC (Supplementary Fig. 5c, d), but exposure of these mice to an HFHS aggravated systemic glucose disposal and decreased insulin secretion after glucose challenge (Fig. 4e, f). Accordingly, islet hyperplasia and the number of Ki67-positive cells decreased slightly but significantly in  $\beta$ *Erbb3*KO relative to WT mice (Fig. 4g, h), although serum Neuregulin1 $\alpha$  levels were comparable in HFHS-treated mice, irrespective of pancreatic *Erbb3* gene status (Supplementary Fig. 5e). Importantly, administration of rNRG1 $\alpha$  protein to mice during the last 4 weeks of HFHS treatment (Supplementary Fig. 5a) did not rescue phenotypes of aggravated systemic glucose tolerance (Supplementary Fig. 5f), impaired islet hyperplasia or decreased Ki-67-positive cell numbers in  $\beta$ *Erbb3*KO mice (Supplementary Fig. 5g, h). These findings indicate that ERBB3 likely serves as a Neuregulin1 $\alpha$  receptor in the pancreas to stimulate compensatory islet hyperplasia in obese diabetic conditions.

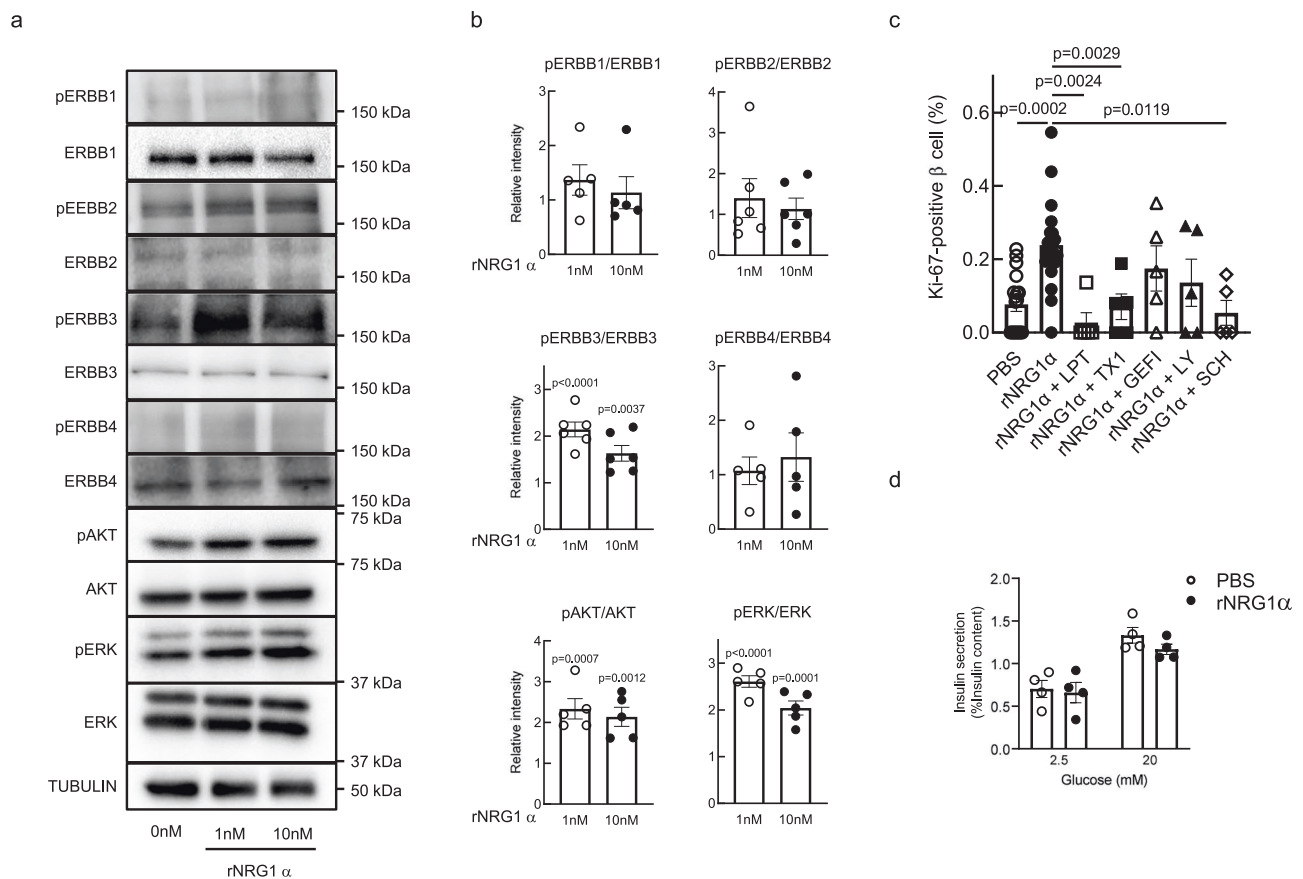


**Fig. 5 | Neuregulin1 promotes  $\beta$  cell proliferation in an ERBB2/3-ERK dependent manner. **a**, **b** Immunoblots (**a**) and corresponding quantification (**b**) of total and phosphorylated forms of ERBBs, AKT, and ERK in MIN6 cells treated with either PBS or indicated concentrations of recombinant protein encompassing the Neuregulin1  $\alpha$  type EGF-like domain (rNRG1 $\alpha$ ) for 30 min. Tubulin served as a loading control. The average value of the ratio of phosphorylated to non-phosphorylated protein in samples from the group treated without rNRG1, normalized by the expression level of TUBULIN, was set to 1. Data represent mean  $\pm$  SEM;  $n = 5$  (pERBB1/ERBB1, pERBB4/ERBB4, pAKT/AKT, and pERK/ERK) and 6 (pERBB2/ERBB2 and pERBB3/ERBB3) per group. The samples derive from the same experiment, and blots were processed in parallel. This experiment was**

repeated at least five times independently. **c** Percentage of Ki-67-positive cells in isolated mouse islets treated with control PBS or rNRG1 $\alpha$  in the absence or presence of indicated inhibitors. Inhibitors were added to the medium 30 min before rNRG1 $\alpha$  stimulation (10 nM, 24 h). LPT: lapatinib, TX1; TX1-85-1, GEF1; gefitinib, LY; LY294002, SCH; SCH772984. Data represent mean  $\pm$  SEM;  $n = 18$  (PBS), 19 (rNRG1 $\alpha$ ), and 5 (rNRG1 $\alpha$  plus each inhibitor) islets per group. **d** Glucose-stimulated insulin secretion. Islets were stimulated for 1 h with either low (2.5 mM) or high (25 mM) glucose in the absence or presence of rNRG1 $\alpha$  (10 nM). Data represent mean  $\pm$  SEM;  $n = 4$  islets per group. No statistically significant differences were found between the two groups. An unpaired Student's  $t$  test (**b**, **d**) and a one-way ANOVA (**c**) were performed.

ERBB receptors transmit external signals by forming functional dimers that activate two major intracellular signaling cascades: the PI3K (Phosphoinositide 3-kinase)/AKT (AKT Serine/Threonine Kinase) and MEK (mitogen-activated protein kinase kinase)/ERK (extracellular signal-regulated kinase) pathways<sup>12</sup>. Therefore, we asked which pathway mediates ERBB3 signaling associated with Neuregulin1 $\alpha$ -mediated  $\beta$  cell proliferation. When we stimulated the mouse  $\beta$  cell line MIN6 with rNRG1 $\alpha$ , among ERBBs, only ERBB3 showed upregulated phosphorylation accompanied by increased phosphorylation of both ERK and AKT (Fig. 5a, b). In contrast, rNRG1 $\alpha$  injection into normal mice promoted phosphorylation of ERBB2, but not ERBB1 and ERBB4, with marked activation of ERBB3 in the pancreas (Fig. 4a, b). We also observed substantial phosphorylation of ERK, but not AKT, in the pancreas in response to rNRG1 $\alpha$  treatment (Fig. 4a, b) and increased phosphorylated ERK in the pancreas of mice fed an HFHS (Fig. 4c, d) in vivo. To assess whether ERBB2/3 heterodimers and MEK/ERK signaling were important in regulating Neuregulin1 $\alpha$ -mediated  $\beta$  cell proliferation, we stimulated mouse primary islets with rNRG1 $\alpha$  protein in vitro and observed a marked increase in the number of Ki-67-positive  $\beta$  cells relative to controls (Fig. 5c), responses completely abolished by treatment of islets with lapatinib (an ERBB1/2 inhibitor) or TX1-85-1 (a specific ERBB3 inhibitor). On the other hand, the ERBB1

inhibitor gefitinib had no effect on Neuregulin1 $\alpha$ -stimulated proliferative responses (Fig. 5c). SCH772984 (a specific ERK1/2 inhibitor) also completely abolished Neuregulin1 $\alpha$ -mediated responses, whereas treatment with LY294002 (an inhibitor of PI3K) minimally decreased Neuregulin1 $\alpha$ -mediated responses (Fig. 5c). By contrast, rNRG1 $\alpha$  treatment did not alter either basal or glucose-stimulated insulin secretion (Fig. 5d). Collectively, these results strongly suggest that Neuregulin1 $\alpha$  stimulates pancreatic  $\beta$  cell proliferation by activating ERBB2/3 receptors and downstream ERK kinase.

### Serum Neuregulin1 $\alpha$ levels increase in MASLD patients

We next investigated the clinical relevance to humans of Neuregulin1 $\alpha$  as a hepatokine using cultures of PXB cells, which consist of >90% normal human hepatocytes isolated from humanized mouse liver<sup>15</sup>. We detected Neuregulin1 $\alpha$  protein in the culture medium of PXB cells (Fig. 6a), although its molecular weight was greater than that of mouse Neuregulin1 $\alpha$ . Mice fed an HFHS diet exhibited obesity and fatty liver followed by diabetes (Supplementary Fig. 1b–d), suggesting that aberrant lipid accumulation in the liver promotes induction of hepatic *type I Neuregulin1 $\alpha$*  expression. Therefore, we analyzed liver and serum samples of patients with MASLD<sup>16</sup> to assess a potential correlation between serum levels of Neuregulin1 $\alpha$  protein and hepatic *type I*

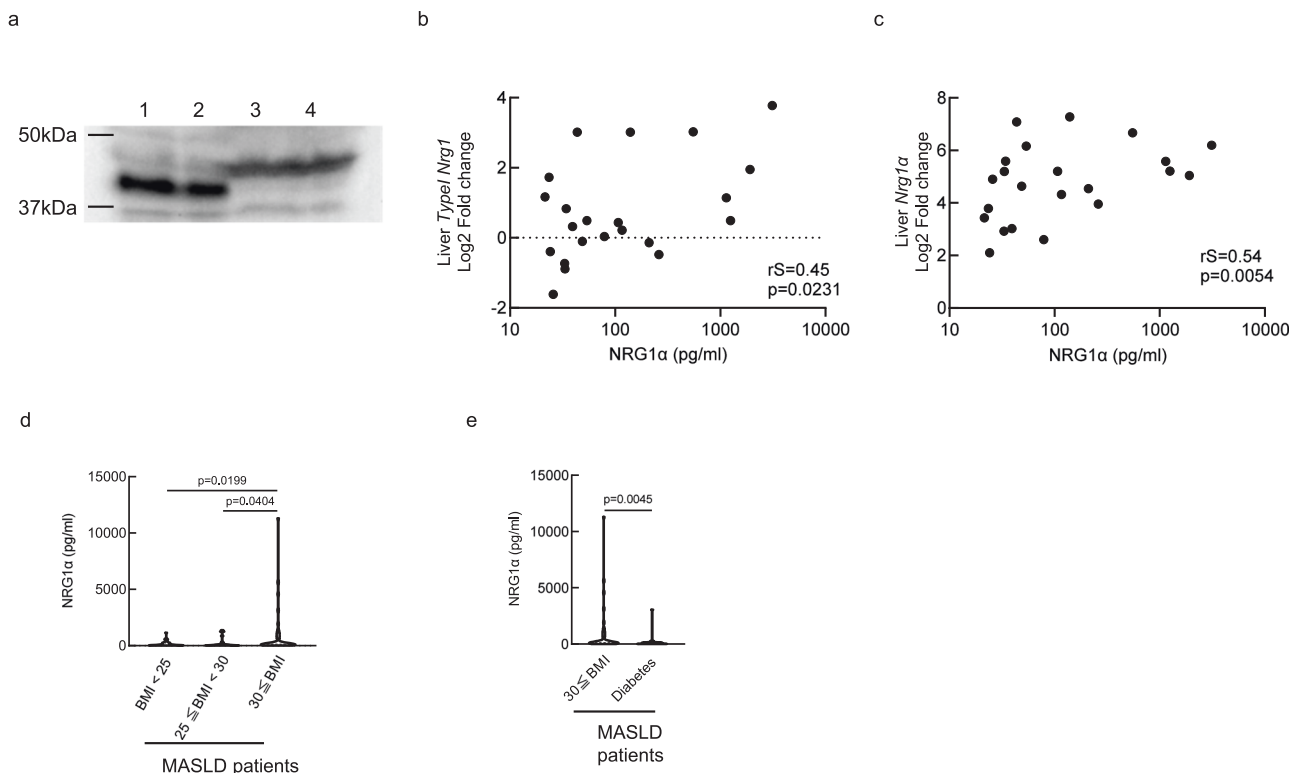


**Fig. 6 | Serum Neuregulin1α levels increase in MASLD human subjects with obesity.** **a** Immunoblotting of Neuregulin1α in culture medium from isolated hepatocytes. Lanes 1&2, 16, and 8 μl of 100 x concentrated culture medium from mouse hepatocytes ( $3.5 \times 10^5$  cells/mL); Lanes 3&4, 16, and 8 μl of 100 x concentrated culture medium from human hepatocytes ( $7.6 \times 10^5$  cells/mL) isolated from PXB mice. This experiment was repeated twice independently. **b, c** Correlation of levels of hepatic *type I Neuregulin1 (Nrg1)* mRNA with serum Neuregulin1α protein (NRG1α) (**b**), and hepatic *Neuregulin1α* mRNA with serum NRG1α (**c**) from metabolic dysfunction associated steatotic liver disease (MASLD)

patients.  $\chi^2$  tests were used for statistical analysis.  $n = 25$ . **d, e** Levels of serum Neuregulin1α from MASLD patients. **d**: comparison of serum NRG1α levels among MASLD patients. The MASLD group was divided into three groups depending on obesity. **e**: comparison of serum Neuregulin1α levels in MASLD patients with obesity and diabetes.  $n = 36$  (BMI < 25), 36 ( $25 \leq \text{BMI} < 30$ ), 42 ( $30 \leq \text{BMI}$ ), and 38 (diabetes) individuals with MASLD per group. Single regression analysis (two-tailed Spearman's correlation coefficient) (**b, c**), a Kruskal-Wallis test (**d**), and a two-tailed Mann-Whitney U test (**e**) were performed.

*Neuregulin1α* expression. As expected, expression levels of both *type I Neuregulin1* and *Neuregulin1α* in the human liver were positively correlated with serum Neuregulin1α protein levels (Fig. 6b, c, Supplementary Table 3), suggesting that the human liver is a major source of Neuregulin1α released into the bloodstream.

Next, we assessed serum Neuregulin1α levels in both MASLD patients with normal weight (BMI < 25) ( $N = 35$ ,  $144.0 \pm 40.59$  pg/ml) and healthy volunteers ( $N = 10$ ,  $94.3 \pm 35.11$  pg/ml) and found those levels to be highly variable: about half of the samples were below detection limit but some samples showed levels above a few hundred pg/ml (Fig. 6d). However, when we analyzed MASLD patients with obesity (BMI ≥ 30) and without diabetes, their serum Neuregulin1α levels significantly increase (Fig. 6d,  $N = 42$ ,  $837.8 \pm 315.0$  pg/ml) when compared to both normal weight (BMI < 25) and overweight ( $25 \leq \text{BMI} < 30$ ,  $N = 36$ ,  $177.5 \pm 61.81$  pg/ml) MASLD subjects without diabetes (Supplementary Table 4). In addition, we also found a weak, but significant positive correlation between serum Neuregulin1α levels and BMI in MASLD patients without T2D (Supplementary Fig. 6a). By contrast, there is no correlation between serum Neuregulin1α levels and fasting insulin levels, fasting blood glucose levels or HbA1c levels, respectively, in MASLD patients without diabetes (Supplementary Fig. 6b–d and Supplementary Table 4). In addition, liver stiffness also did not correlate with serum Neuregulin1α levels, although patients with liver fibrosis showed a trend towards lower serum Neuregulin1α levels when compared to those without liver fibrosis (Supplementary Fig. 6e, f and Supplementary Table 5, 6). Interestingly, when we analyzed T2D patients with MASLD and compared to MASLD patients with

obesity and without diabetes, their serum Neuregulin1α levels were unexpectedly low, whether they exhibited obesity or not (Fig. 6e and Supplementary Table 4,  $N = 38$ ,  $150.6 \pm 79.45$  pg/ml), suggesting that Neuregulin1α may inhibit development of T2D in MASLD patients.

## Discussion

Compensatory  $\beta$  cell proliferation accompanies insulin resistance to meet increased systemic insulin demand and thus serves to prevent T2D by enhancing insulin secretion. Circulating factors released from peripheral cells and organs are implicated in this compensatory response in diverse states of insulin-resistance<sup>17–21</sup>, and the liver is known to be a major source of these factors, among them, serpinB1 and hepatocyte growth factor<sup>8,9,22</sup>. However, whether other liver-derived secretory proteins contribute to compensatory  $\beta$  cell proliferation has not been fully investigated. In this study, we searched for other such candidate(s) by analyzing changes in hepatic gene expression and islet size over time in mice fed an HFHS. That analysis identified type I Neuregulin1α as a hepatokine that promotes  $\beta$  cell proliferation.

We and others previously reported that Neuregulin1 enhances systemic glucose disposal, in part by suppressing hepatic gluconeogenesis<sup>10,23,24</sup>. This is in contrast to our present findings showing that Neuregulin1α increases insulin secretion by stimulating  $\beta$  cell proliferation in an endocrine manner. At present, we cannot explain why we did not observe changes in hepatic gluconeogenic activity or expression of the gluconeogenic genes in mice fed an HFHS for 15 weeks after *Neuregulin1α* deletion or overexpression in the liver.

However, given that chronic exposure to Neuregulin1 $\beta$  attenuates insulin secretion likely due to improved systemic glucose tolerance in diabetic mice<sup>23,25</sup>, these differences could be attributable to isoform-specific functions of Neuregulin1 on pancreatic  $\beta$  cells, suggesting the functional importance of Neuregulin1 $\alpha$  domain products for islet hyperplasia. This idea is supported by findings reported here that administration of rNRG1 $\alpha$  protein stimulated  $\beta$  cell expansion without altering hepatic gluconeogenic gene expression in normal or diabetic mice. In addition, our present results showing a positive correlation between serum Neuregulin1 $\alpha$  levels and islet size in mice fed an HFHS diet further support the importance of Neuregulin1 $\alpha$  as an endogenous activator of pancreatic  $\beta$  cell proliferation, although a substantial increase in serum Neuregulin1 $\alpha$  levels for at least a few weeks is likely to be a prerequisite for exerting its effects on pancreatic  $\beta$  cells. Activation of intra-pancreatic Neuregulin1-ERBB signaling reportedly elicits  $\beta$  cell regeneration in the severely damaged pancreas of *Arid1a*-deficient mice<sup>26</sup>. However, as *Neuregulin1* expression was only altered in the liver by exposure to an HFHS, and increased serum Neuregulin1 $\alpha$  levels were completely abolished in liver-specific *Neuregulin1*-deficient diabetic mice, we propose that the liver is the main source of circulating Neuregulin1 $\alpha$ , thereby creating communication between liver and pancreas to drive compensatory  $\beta$  cell expansion in diabetic conditions. Although further investigation is needed to define molecular mechanisms conferring selectivity of Neuregulin1 $\alpha$  targeting to pancreatic  $\beta$  cells and to examine the effects of disease conditions on the cleavage and secretion of hepatic Neuregulin1 $\alpha$ , these results indicate the significance of Neuregulin1 $\alpha$  as a liver-derived endogenous humoral factor that stimulates  $\beta$  cell proliferation and prevents T2D disease progression.

Neuregulin1 binds to either ERBB3 or ERBB4 and forms either homo or heterodimers with other ERBBs on target cells<sup>12</sup>. Global *ErbB3* deletion impairs normal  $\beta$  cell development in mice<sup>14</sup>, and genome-wide association studies have identified a strong association between *ERBB3* and type 1 diabetes<sup>27,28</sup>, indicating the importance of ERBB3 in pancreatic  $\beta$  cell biology. Although ERBB3 and ERBB4 are reportedly expressed to varying degrees in human and mouse adult pancreas<sup>29–32</sup>, Neuregulin1 $\alpha$  activates ERBB3 preferentially to stimulate  $\beta$  cell proliferation, and the selective ERBB3 inhibitor TX1-85-1 completely abolishes Neuregulin1 $\alpha$ -mediated  $\beta$  cell proliferation in vitro. Accordingly, we found that *ErbB3* loss in adult pancreas abrogated compensatory islet hyperplasia in diabetic mice, a response not rescued by treatment with rNRG1 $\alpha$  protein, indicating the crucial role of Neuregulin1-ERBB3 signaling in regulating compensatory  $\beta$  cell expansion. Since ERBB3 lacks intrinsic kinase activity<sup>33</sup>, other ERBBs are likely required to form dimers that activate Neuregulin1 $\alpha$ -mediated downstream signaling. Treatment with lapatinib, a selective inhibitor of both ERBB1 and ERBB2, but not gefitinib, which is a specific ERBB1 inhibitor, completely abrogated Neuregulin1 $\alpha$ -mediated  $\beta$  cell proliferation in isolated mouse islets. In agreement with these results, Neuregulin1 $\alpha$  reportedly shows the highest affinity for ERBB2/3 complexes among sets of dimeric ERBB combinations<sup>34</sup>, and, in our study, both ERBB2 and ERBB3 in mouse pancreas were phosphorylated in response to rNRG1 $\alpha$ , suggesting that ERBB2/3 receptors are required for Neuregulin1 $\alpha$ -mediated  $\beta$  cell proliferation.

We also showed that treatment of primary mouse islets with the specific ERK1/2 inhibitor SCH772984 significantly blunted Neuregulin1 $\alpha$ -mediated  $\beta$  cell proliferation, while treatment with the PI3K inhibitor LY294002 did not. These results suggest that Neuregulin1 $\alpha$  selectively activates MEK/ERK signaling to promote  $\beta$  cell proliferation without altering glucose-stimulated insulin secretion, although ERBB2/3 complexes can activate both PI3K/AKT and MEK/ERK signaling involved in regulating  $\beta$  cell mass and insulin secretion<sup>35–39</sup>. Here, we cannot rule out the potential involvement of PI3K/AKT signaling in regulating of Neuregulin1 $\alpha$ -mediated compensatory  $\beta$  cell proliferation in vivo. However, considering that the insulin receptor signaling cascade,

including PI3K/AKT, is attenuated in diabetic islets<sup>40,41</sup>, selective activation of MEK/ERK by Neuregulin1 $\alpha$  would provide an alternative strategy to expand even insulin-resistant  $\beta$  cells. Accordingly, pancreatic MEK/ERK activity is reportedly preserved and can induce compensatory islet hyperplasia in diet-induced obese mice<sup>36,38,39,42</sup>. Overall, our present data indicate that the Neuregulin1 $\alpha$ -ERBB3-ERK signaling pathway plays crucial roles in compensatory islet hyperplasia in obese, diabetic conditions.

The clinical relevance of circulating Neuregulin1 $\beta$  to both cardiovascular disease and schizophrenia has been extensively investigated<sup>43–47</sup>, whereas information relevant to Neuregulin1 $\alpha$  activity is limited. Although circulating Neuregulin1 $\alpha$  levels are much lower than those of Neuregulin1 $\beta$ , we found serum Neuregulin1 $\alpha$  levels to be positively correlated with hepatic *type 1 Neuregulin1 $\alpha$*  expression in MASLD patients, suggesting that, as in mouse, human liver is a major organ that releases Neuregulin1 $\alpha$  into the blood, where it serves as a hepatokine. Accordingly, we show that isolated human hepatocytes secrete the Neuregulin1 $\alpha$  extracellular domain into the culture medium.

In this study, we were unable to match age, gender, or body mass index among patients and healthy volunteers when assessing serum Neuregulin1 $\alpha$  levels due to limited sample sizes. However, our data suggests that higher serum Neuregulin1 $\alpha$  levels in MASLD subjects mirror obesity and support the idea that peripheral insulin resistance evokes compensatory islet hyperplasia, in part, by increasing circulating Neuregulin1 $\alpha$  levels. Of note, we found that T2D patients with MASLD show markedly reduced serum Neuregulin1 $\alpha$  levels relative to MASLD patients with a BMI  $\geq 30$ . These findings may indicate exhaustion of the liver's capacity to respond to T2D progression and that decreased circulating Neuregulin1 $\alpha$  levels may trigger T2D onset by impairing compensatory islet hyperplasia. Another explanation can also account for the decreased circulating Neuregulin1 $\alpha$  levels in T2D patients with MASLD: a sustained elevation of serum Neuregulin1 $\alpha$  in response to sustained metabolic stress may accelerate the onset and progression of T2D by stimulating  $\beta$  cell proliferation over an extended period, thereby promoting pancreatic  $\beta$  cell exhaustion. On the other hand, as higher concentrations of circulating Neuregulin1 $\alpha$  were positively associated with islet hyperplasia in obese diabetic mice, Neuregulin1 $\alpha$  may serve as a biomarker of functional  $\beta$  cell mass and be useful in distinguishing between compensated and decompensated  $\beta$  cell failure in diabetes. Further studies are needed to determine whether Neuregulin1 $\alpha$  stimulates human  $\beta$  cell proliferation and whether circulating Neuregulin1 $\alpha$  levels correlate positively with functional  $\beta$  cell mass.

In conclusion, we identified Neuregulin1 $\alpha$  as a liver-derived secretory protein that promotes  $\beta$  cell proliferation via activating ERBB3-ERK signaling and stimulating systemic glucose disposal with increased insulin secretion. Our study deepens our knowledge of how liver functions as a central organ to regulate systemic glucose metabolism via the secretory protein, Neuregulin1 $\alpha$ , and may pave the way for developing therapeutic strategies to target Neuregulin1 $\alpha$  and restore functional  $\beta$  cell mass in T2D.

## Methods

All experiments were conducted in accordance with Waseda University Animal Welfare Guidelines and approved by the Animal Experimentation Committee of the Waseda University (2020-A063, A2021-A039, A22-047, A23-059, A24-070).

## Animal studies

C57BL/6 mice and *ob/ob* mice were purchased from The Jackson Laboratory (Bar Harbor, ME). Alb-Cre::*Nrg1*<sup>fllox/fllox</sup> mice (hereafter referred to as LN*Nrg1*KO mice) were generated by crossing *Nrg1*<sup>fllox/fllox</sup> mutant mice and Alb-Cre transgenic mice. Pdx1-CreERT::*ErbB3*<sup>fllox/fllox</sup> mice were produced by breeding *ErbB3*<sup>fllox/fllox</sup> mice purchased from



Mutant Mouse Resource and Research Centers at UNC with Pdx1-CreERT transgenic mice, kindly provided by Prof. Guoqiang Gu (Vanderbilt University School of Medicine)<sup>13</sup>. Pancreatic  $\beta$  cell-specific deletion of *ErbB3* was induced by IP injection of 2 mg tamoxifen (#128654, Fujifilm Wako Pure Chemical, Osaka, Japan) into Pdx1-CreERT::*ErbB3*<sup>fllox/flox</sup> mice (hereafter referred to as  $\beta$ *ErbB3*KO mice, 5 weeks of age) for 3 consecutive days. Pdx1-CreERT::*ErbB3*<sup>fllox/flox</sup> mice treated with corn oil (#032-17016, Fujifilm Wako Pure Chemical) instead of tamoxifen served as controls. All male mice used in our experiments were maintained in the animal facility at TWIns of Waseda University with a 12 h light cycle and free access to water and chow (Labo MR stock, #644352, Nosan, Yokohama, Japan). The ambient conditions of the animal facilities were set at 22 °C and 45% humidity. Feeding with a high-fat, high-sucrose diet (HFHS diet, consisting of 20.7% lard, 46.5% sucrose, 17.1% milk casein, 4.78% crystalline cellulose, 4.56% corn starch, 1.54%  $\alpha$ -corn starch, 0.24% L-cystine, 0.24% choline bitartrate, 0.0041% tertiary butylhydroquinone, 3.35% AIN-93M, 0.96% AIN-93, blended by CLEA Japan, Tokyo, Japan) was started at either 5 weeks (C57BL/6, *LNrg1*KO, and respective control mice) or 1 week after the last tamoxifen injection (6 weeks of age;  $\beta$ *ErbB3*KO and respective control mice) for 15 weeks (Supplementary Figs. 1a, 2a, 4a, 5a and Supplementary Table 1). Mouse blood and tissues were collected from overnight-fasted mice and immediately frozen in liquid nitrogen for further measurements, unless otherwise noted. Only male mice were used in experiments.

### Genotyping

All transgenic mice were genotyped using PCR-based assays of tail DNA as following. The PCR protocol used to genotype Alb-Cre::*Nrg1*<sup>fllox/flox</sup> mice and Pdx1-CreERT::*ErbB3*<sup>fllox/flox</sup> mice was as follows: 97 °C, 3 min, 30 cycles (95 °C, 30 s; 60 °C, 30 s; 72 °C, 60 s), and 4 °C hold for Alb-Cre::*Nrg1*<sup>fllox/flox</sup> mice; and 97 °C, 3 min, 30 cycles (95 °C, 30 s; 58 °C, 30 s; 72 °C, 40 s), and 4 °C hold for Pdx1-CreERT::*ErbB3*<sup>fllox/flox</sup> mice. Primers used are listed in Supplementary Table 2.

### OGTT, PTT and ITT

Oral glucose tolerance tests (OGTT, 2 mg/g body weight, by oral gavage), pyruvate tolerance tests (PTT, 2 mg/g body weight, IP), and insulin tolerance tests (ITT, 0.75 IU/kg body weight, IP) were performed in mice fasted for 16, 24, and 6 h, respectively. Blood was collected from the tail vein at 0, 15, 30, 60, 90, and 120 min after administration of either glucose, pyruvate, or insulin (Humulin® R, #87 2492, Eli Lilly Japan, Kobe, Japan) and blood glucose was determined using an Accu-chek ST meter (Roche DC Japan, Tokyo, Japan). Blood collected at 0, 15, 30, and 60 min during OGTT was also used to measure serum insulin using an ultra-sensitive mouse insulin ELISA kit (#M1104, Morinaga Institute of Biological Science, Yokohama, Japan). Detail information about treatments, mouse strains/genotypes, and age and a number of mice were listed in Supplementary Table 1.

### ELISA

Serum insulin and plasma NRG1 $\alpha$  were determined using an ultra-sensitive mouse insulin ELISA kit (#M1104, Morinaga Institute of Biological Science) and human NRG1- $\alpha$ /HRG1- $\alpha$  ELISA (#ELH-NRG1 $\alpha$ -1, Raybiotech Life, Peachtree Corners, GA), respectively. Blood was collected from the heart at the sacrifice of overnight-fasted mice and from the median mesothelial vein of humans after overnight fasting.

### Tissue sampling

To confirm insulin resistance evoked by feeding an HFHS diet, the liver, quadriceps skeletal muscle, and epididymal adipose tissues of mice fed an HFHS diet for 15 weeks were collected 15 min after insulin administration (0.75 IU/kg body weight, IP) (Supplementary Table 1).

### Preparation of a recombinant NRG1 $\alpha$ protein and animal treatment

A partially purified recombinant protein fragment (rNRG1 $\alpha$ ) encompassing His171 to Arg242 of the mouse NRG1 $\alpha$  protein (rNRG1 $\alpha$ ) was prepared using pCold I vector (#3361, Takara Bio, Kusatsu, Japan), a HisTALON Gravity Column Purification Kit (#635654, Takara Bio), and a High Capacity Endotoxin Removal Spin Column (#88276, Thermo Fisher Scientific, Waltham, MA)<sup>10</sup>. Recombinant mouse NRG1 $\alpha$  protein (rNRG1 $\alpha$ , 100 ng/g body weight) was injected IP into mice (C57BL/6 mice fed an NC) one time 30 min before sampling (Fig. 4a, b and Supplementary Table 1) or 3 times a week for last 4 or 5 weeks before sampling (C57BL/6 mice and *ob/ob* mice fed an NC in Fig. 3 and Supplementary Fig. 3, and  $\beta$ *ErbB3*KO mice fed an HFHS in Supplementary Fig. 5a, e—hand Supplementary Table 1).

### Adeno-associated virus (AAV) preparation and animal treatment

HEK293T cells (ATCC, CRL-3216) were transfected with a mixture of p5E18-VD2/8-AAV capsid 8 plasmid (provided from Penn Vector Core), AAV helper plasmid XX6-80 (from UNC-Chapel Hill) and pAAV2-LSP1 EGFP (from Children's Medical Research Institute, New South Wales, Australia) or pAAV2-LSP1 Type I neuregulin1 $\alpha$  (at a ratio of 1:1:2) using polyethylenimine. Forty-eight hours later, cells were lysed by 4 freeze-thaw cycles to extract AAV particles. Adeno-associated virus serotype 8 (AAV8,  $1 \times 10^{10}$  vg/kg body weight), driven by the ApoE enhancer and hAAT promoter, was administered IP one time to mice that had already been fed an HFHS for 10 weeks and were then subjected to another 5 weeks of HFHS (Supplementary Fig. 4a and Supplementary Table 1).

### RNA isolation, Quantitative PCR analysis and DNA microarray analyses

Total RNA was isolated from frozen mouse and human tissues using RNeasy Plus (#9109, Takara Bio). cDNA was synthesized from total RNA using a ReverTra Ace (#TRT-101, TOYOBO, Osaka, Japan). Conventional PCR was performed using specific primer sets (Supplementary Table 2) to identify *Nrg1 $\alpha$*  isoforms expressed in mouse liver. Transcript levels were measured with GoTaq qPCR Master Mix (#A6001, Promega, Madison, WI) using primer sets and comparisons with target genes listed in Supplementary Table 2. As an internal control gene, expression levels were normalized to *18S rRNA* in mouse experiments. In human studies,  $\beta$ -actin served as an internal control. Equal amounts of total RNA isolated from livers of 4 mice each fed an HFHS diet for 0, 5, 10, or 15 weeks were mixed and subjected to analysis with a 8x60K Agilent Whole Mouse Genome 44 K Oligo Microarray (Agilent Technology, Santa Clara, CA) to determine relative gene expression levels.

### Cell culture and treatments

MIN6 cells (ATCC, CRL-11506) were maintained in DMEM (#043-30085, Fujifilm Wako Pure Chemical) with 12.5% fetal bovine serum (Biosera, Cholet, France), 20 mM HEPES, 5.5  $\mu$ M 2-mecrptoethanol (#131-14572, Fujifilm Wako Pure Chemical), 100 units/mL penicillin, and 0.1 mg/mL streptomycin (#15070-063, Thermo Fisher Scientific) in humidified 5% CO<sub>2</sub> at 37 °C. After being incubated in fetal bovine serum-free medium overnight, cells were stimulated 30 min with 1 or 10 nM rNRG1 $\alpha$  (Supplementary Table 1) and subjected to immunoblotting analysis. Primary mouse hepatocytes ( $3.5 \times 10^5$  cells/mL) were isolated and cultured in William's medium E (#12551032, Thermo Fisher Scientific) supplemented with 10% fetal bovine serum (Biosera) at 37 °C in 5% CO<sub>2</sub>. PXB-cells ( $7.6 \times 10^5$  cells/mL, Cat #: PPC-T25), which are primary human normal hepatocytes, were purchased from PhoenixBio Co., Ltd (Hiroshima, Japan). Hepatocytes were cultured for 48 h in serum-free DMEM. Conditioned medium was then collected and analyzed for NRG1 $\alpha$  protein (Supplementary Table 1).

## Islet studies

Collagenase solution (2 mg/ml dissolved in HBSS, #032-22364, Fujifilm Wako Pure Chemical) was administered from the common bile duct into the mouse pancreas, after which the pancreas was excised and was further digested for 15–20 min at 37 °C. Islets were washed twice with HBSS (#084-08345, Fujifilm Wako Pure Chemical) and then separated by Percoll (#17-0891-01, Cytiva, Tokyo, Japan) density gradient centrifugation. Islets were manually picked and maintained in RPMI 1640 medium (#1060122, Fujifilm Wako Pure Chemical) containing 10% FBS (Biosera), 100 units/ml penicillin, and 0.1 mg/ml streptomycin (Thermo Fisher Scientific) for further experiments. For proliferation analysis, islets were stimulated with 10 nM rNRG1 $\alpha$  every 12 h for 24 h after pre-incubation with serum-free RPMI1640 medium and then immunostained with anti-Ki-67 antibody (Supplementary Table 1). In some experiments, an inhibitor (LPT, 1  $\mu$ M lapatinib (#SML2259, Sigma-Aldrich, St. Louis, MO); TXI, 2  $\mu$ M TXI-85-1 (#HY-10084, MedChemExpress, Monmouth Junction, NJ); GEFI, 1  $\mu$ M gefitinib (#078-06561, Fujifilm Wako Pure Chemical); LY, 50  $\mu$ M LY294002 (#129-04861, Fujifilm Wako Pure Chemical); or SCH, 3  $\mu$ M SCH772984 (#HY-5084, MedChemExpress)) was added to the medium 30 min before rNRG1 $\alpha$  stimulation (Supplementary Table 1). For glucose-stimulated insulin secretion analysis, islets were incubated 1 h with either 2.5 or 20 mM glucose-containing RPMI 1640 medium, with or without 10 nM rNRG1 $\alpha$  (Supplementary Table 1). Islets were extracted with 75% acid ethanol, and insulin concentrations were measured using an ultra-sensitive mouse insulin ELISA kit (#M1104, Morinaga Institute of Biological Science). To determine the deletion efficiency of the *ErbB3* gene in tamoxifen-treated Pdx1-CreERT::*ErbB3*<sup>fllox/fllox</sup> mice, genomic PCR was performed on genomic DNA extracted from isolated islets using Wizard® Genomic DNA Purification Kit (#A1120, Promega). PCR protocol and primers were as follows: 94 °C, 2 min, 30 cycles (98 °C, 10 s; 63 °C, 30 s; 68 °C, 30 s), 68 °C, 5 min, and 4 °C hold, and forward primer; 5'-TGTGCTAGCCCAAGAGATG-3', and reverse primer; 5'-ACA-TAACCTGGTTACAGGACC-3'.

## Western blot analyses

To prepare total lysates, tissues and cells frozen in liquid nitrogen were homogenized in lysis buffer containing 20 mM HEPES (pH 7.9), 0.5% deoxycholate, 1% NP-40, 0.1% SDS, 20% glycerol, 150 mM NaCl, 1 mM MgCl<sub>2</sub>, 5 mM NaF, 1 mM sodium orthovanadate, 1 mM DTT, 0.5 mM EDTA, 0.1 mM EGTA, and a protease inhibitor cocktail (#P8340, Sigma-Aldrich, St. Louis, MO). Hundred-fold concentrated samples of conditioned medium were prepared by centrifugal ultrafiltration (vivaspin 6, # 28932296, Cytiva). Western blotting of 50–100  $\mu$ g protein from total lysates was performed using a specific antibody against each target protein listed below. Signals were detected by using Immobilon Western Chemiluminescent HRP Substrate (#WBKLS, Millipore-Sigma, Burlington, MA).

## Antibodies and reagents

Primary antibodies to AKT (#4691, 1:1000), phospho-AKT (ser473) (#4060, 1:1000), p44/42 MAPK (ERK1/2) (#4695, 1:1000), phospho-p44/42 MAPK (ERK1/2) (Thr202/Tyr204) (#4370, 1:1000), EGFR (#4267, 1:1000), phospho-EGFR (Tyr1068) (#3777, 1:1000), HER2/ERBB2 (#4290, 1:1000), phospho-HER2/ERBB2 (Tyr1221/1222) (#2243, 1:1000), HER3/ERBB3 (#12708, 1:1000), phospho-HER3/ERBB3 (Tyr1289) (#2842, 1:1000), HER4/ERBB4 (#4795, 1:1000), phospho-HER4/ERBB4 (Tyr1284/1173) (#4757, 1:1000), Ki-67 (for immunohistochemical analysis, #12202, 1:400 and for immunofluorescence analysis, #9129, 1:400) were purchased from Cell Signaling Technology (Beverly, MA); INSULIN (#12018, 1:1000), GLUCAGON (for immunohistochemical analysis, #G2654, 1:1000),  $\alpha$ -TUBULIN (#T9026, 1:1000) were from Sigma-Aldrich; GLUCAGON (for immunofluorescence analysis, #10505, 1:500) and Pancreatic Polypeptide (for immunofluorescence analysis, #10501, 1:200) were from IBL (Gunma, Japan);

NRG1- $\alpha$ /HRG1- $\alpha$  (#AF-296-NA, 1:1000) was from R&D Systems (Minneapolis, MN),  $\beta$ -ACTIN conjugated with HRP (sc-47778HRP, 1:100,000) was from Santa Cruz (Dalla, TX). Donkey anti Rabbit IgG, HRP-linked F(ab')<sub>2</sub> fragment (NA9340, 1:10000, Cytiva), Horse anti-mouse IgG, HRP-linked antibody (#7076, Cell Signaling Technology, 1:3000), and Rabbit HRP-conjugated anti Goat IgG(H+L) Ab (SA00001-4, 1:10000, Proteintech Japan, Tokyo) were used as secondary antibodies for Western blot analysis. Goat Anti-Rabbit IgG Antibody (H+L), Biotinylated (BA-1000-1.5, 1:200) and M.O.M.® (Mouse on Mouse) Biotinylated Anti-Mouse IgG Reagent (MKB-2225-1, 1:250) were purchased from Vector Laboratories (Newark, CA) and used as secondary antibodies for immunohistochemical analysis. Goat anti-Mouse IgG (H+L) Superclonal Secondary Ab, Alexa Fluor 488 (#A28175, 1:200), Goat anti-Rabbit IgG (H+L) Cross-Absorbed Secondary Ab, Alexa Fluor 555 (#A-21428, 1:200), and Goat anti-Rat IgG (H+L) Cross-Absorbed Secondary Ab, Alexa Fluor 647 (#A-21247, 1:200) were purchased from Thermo Fisher Scientific and used as secondary antibodies for immunofluorescence analysis. All other biochemical reagents were purchased from Fujifilm Wako Pure Chemical or Sigma-Aldrich unless otherwise noted.

## Histology, immunohistochemistry, and immunofluorescence

Mouse tissues (pancreas and liver) and primary cultured mouse islets were fixed overnight in 4% paraformaldehyde in phosphate buffer and paraffin-embedded. Five-micrometer-thick sections were then stained with H.E. to measure islet size. In immunohistochemical analyses, serial sections from mice treated with either an HFHS diet, rNRG1 $\alpha$ , or *Nrg1 $\alpha$*  AAV8 were immunostained with anti Ki-67, anti insulin, or anti glucagon antibodies. Using 5–6 serial sections of the mouse pancreas cut every 50  $\mu$ m, the islet size (of at least 500 islets) in each mouse was measured using Photoshop. For immunofluorescence analyses, sections were stained with anti Ki-67, anti-insulin, and anti-glucagon antibodies or Ki-67, anti-pancreatic polypeptide, and anti-glucagon antibodies, simultaneously. Images were captured using cellSens (Olympus, Tokyo, Japan, for H.E. staining and immunohistochemical analyses) or FV3000 (Olympus, for immunofluorescence analyses). Counting of Ki-67-positive  $\beta$  cells (defined as proliferating) was manually carried out or performed using ImageJ in a blinded fashion.

## Human studies

This study was conducted in keeping Helsinki Declaration and with the approval of ethics committees for clinical research at Osaka City University (Number:3641). Written informed consent was provided from all participants. Participants included both males and females over the age of 18 years. Patients who had previously received recombinant insulin therapy were excluded. A total of 257 subjects consisted of MASLD patients who consume small amounts of alcohol per week (~140 g/wk and ~210 g/wk from females and males, respectively) and have at least 1 of 5 cardiometabolic factors<sup>16</sup> visiting the hepato-biliary-pancreatic disease section of the Internal Medicine Department of Osaka City University as well as healthy volunteers (Supplementary Table 3–6). Liver steatosis was diagnosed via abdominal ultrasonography using a Toshiba Aplio 500 Ultrasound Machine (Canon Medical Systems Corporation, Tochigi, Japan). Abdominal ultrasonography was performed by experienced sonographers who were registered with the Japan Society of Ultrasonics in Medicine. Liver steatosis was semi-quantified according to the criteria described by Hamaguchi et al., which are based on the presence of hepatorenal echo contrast, a bright liver, deep attenuation, and vessel blurring<sup>48</sup>. Vibration-Controlled Transient Elastography (VCTE) was carried out using a Fibroscan (EchoSens, Paris, France), and liver fibrosis was diagnosed in patients with a cut-off liver stiffness measurement (LSM) of 8.6 kPa or greater<sup>49</sup> or by histological analysis of the liver biopsy samples. Study participants were analyzed in fasting conditions. Serum NRG1 levels were measured using a Human NRG1-alpha/HRG1-alpha

ELISA kit, as described above. We also correlated serum NRG1 $\alpha$  and hepatic *type I Nrg1 $\alpha$*  expression and other serum parameters, including fasting glucose, fasting insulin, and HbA1c.

### Statistical analysis

Results are shown as means  $\pm$  SEM. Statistical analyses were performed using GraphPad Prism8 software (La Jolla, CA). Statistical comparisons between groups were analyzed for significance using an unpaired two-tailed Student's *t* test and a one-way analysis of variance (ANOVA) with post-hoc Tukey tests as a parametric test, or a Kruskal-Wallis test as a nonparametric test. To correlate hepatic *type I Nrg1 $\alpha$*  mRNA levels, plasma NRG1 $\alpha$  levels and pancreatic islet size of mice and hepatic *type I Nrg1 $\alpha$*  mRNA levels and plasma NRG1 $\alpha$  levels in humans, we carried out single regression analysis with Spearman's correlation coefficient. Statistically significant differences are indicated as \* $P \leq 0.05$ , \*\* $P \leq 0.01$ .

### Reporting summary

Further information on research design is available in the Nature Portfolio Reporting Summary linked to this article.

### Data availability

Microarray data that support the findings of this study have been deposited in GEO with accession number [GSE282007](https://www.ncbi.nlm.nih.gov/geo/query/acc.cgi?acc=GSE282007). All data supporting the findings of this study are available within the paper and its Supplementary Information. Source data are provided in this paper.

### References

- Goldfine, A. B. & Kulkarni, R. N. Modulation of beta-cell function: a translational journey from the bench to the bedside. *Diab. Obes. Metab.* **14**, 152–160 (2012).
- Mezza, T. et al. Beta-cell fate in human insulin resistance and type 2 diabetes: A perspective on islet plasticity. *Diabetes* **68**, 1121–1129 (2019).
- Rines, A. K., Sharabi, K., Tavares, C. D. & Puigserver, P. Targeting hepatic glucose metabolism in the treatment of type 2 diabetes. *Nat. Rev. Drug Discov.* **15**, 786–804 (2016).
- Petersen, M. C., Vatner, D. F. & Shulman, G. I. Regulation of hepatic glucose metabolism in health and disease. *Nat. Rev. Endocrinol.* **13**, 572–587 (2017).
- Stefan, N. & Haring, H. U. The role of hepatokines in metabolism. *Nat. Rev. Endocrinol.* **9**, 144–152 (2013).
- Jensen-Cody, S. O. & Potthoff, M. J. Hepatokines and metabolism: Deciphering communication from the liver. *Mol. Metab.* **44**, 101138 (2021).
- Meex, R. C. et al. Fetuin B is a secreted hepatocyte factor linking steatosis to impaired glucose metabolism. *Cell Metab.* **22**, 1078–1089 (2015).
- El Ouaamari, A. et al. SerpinB1 promotes pancreatic beta cell proliferation. *Cell Metab.* **23**, 194–205 (2016).
- Araujo, T. G. et al. Hepatocyte growth factor plays a key role in insulin resistance-associated compensatory mechanisms. *Endocrinology* **153**, 5760–5769 (2012).
- Arai, T. et al. Type I neuregulin $\alpha$  is a novel local mediator to suppress hepatic gluconeogenesis in mice. *Sci. Rep.* **7**, 42959 (2017).
- Gong, X. M. et al. GpnmB secreted from liver promotes lipogenesis in white adipose tissue and aggravates obesity and insulin resistance. *Nat. Metab.* **1**, 570–583 (2019).
- Mei, L. & Xiong, W. C. Neuregulin 1 in neural development, synaptic plasticity and schizophrenia. *Nat. Rev. Neurosci.* **9**, 437–452 (2008).
- Gu, G., Dubauskaite, J. & Melton, D. A. Direct evidence for the pancreatic lineage: NGN3+ cells are islet progenitors and are distinct from duct progenitors. *Development* **129**, 2447–2457 (2002).
- Erickson, S. L. et al. ErbB3 is required for normal cerebellar and cardiac development: a comparison with ErbB2- and heregulin-deficient mice. *Development* **124**, 4999–5011 (1997).
- Yamasaki, C. et al. Culture density contributes to hepatic functions of fresh human hepatocytes isolated from chimeric mice with humanized livers: Novel, long-term, functional two-dimensional in vitro tool for developing new drugs. *PLoS ONE* **15**, e0237809 (2020).
- Rinella, M. E. et al. A multisociety Delphi consensus statement on new fatty liver disease nomenclature. *J. Hepatol.* **79**, 1542–1556 (2023).
- Flier, S. N., Kulkarni, R. N. & Kahn, C. R. Evidence for a circulating islet cell growth factor in insulin-resistant states. *Proc. Natl. Acad. Sci. USA* **98**, 7475–7480 (2001).
- Kondegowda, N. G. et al. Osteoprotegerin and denosumab stimulate human beta cell proliferation through inhibition of the receptor activator of NF-kappaB ligand pathway. *Cell Metab.* **22**, 77–85 (2015).
- Fernandez-Ruiz, R. et al. Wisp1 is a circulating factor that stimulates proliferation of adult mouse and human beta cells. *Nat. Commun.* **11**, 5982 (2020).
- Prentice, K. J. et al. A hormone complex of FABP4 and nucleoside kinases regulates islet function. *Nature* **600**, 720–726 (2021).
- Lorincz, H., Somodi, S., Ratku, B., Harangi, M. & Paragh, G. Crucial regulatory role of organokines in relation to metabolic changes in non-diabetic obesity. *Metabolites* **13**, 270 (2023).
- El Ouaamari, A. et al. Liver-derived systemic factors drive beta cell hyperplasia in insulin-resistant states. *Cell Rep.* **3**, 401–410 (2013).
- Ennequin, G. et al. Neuregulin 1 improves glucose tolerance in db/db mice. *PLoS ONE* **10**, e0130568 (2015).
- Lopez-Soldado, I. et al. Neuregulin improves response to glucose tolerance test in control and diabetic rats. *Am. J. Physiol. Endocrinol. Metab.* **310**, E440–E451 (2016).
- Ennequin, G. et al. Neuregulin 1 treatment improves glucose tolerance in diabetic db/db mice, but not in healthy mice. *Arch. Physiol. Biochem.* **126**, 320–325 (2018).
- Celen, C. et al. Arid1a loss potentiates pancreatic beta-cell regeneration through activation of EGF signaling. *Cell Rep.* **41**, 111581 (2022).
- Brorsson, C. A., Pociot, F. & Type 1 Diabetes Genetics, C. Shared genetic basis for type 1 diabetes, islet autoantibodies, and autoantibodies associated with other immune-mediated diseases in families with type 1 diabetes. *Diab. Care* **38**, S8–S13 (2015).
- Kaur, S. et al. The genetic and regulatory architecture of ERBB3-type 1 diabetes susceptibility locus. *Mol. Cell Endocrinol.* **419**, 83–91 (2016).
- Miyagawa, J. et al. Immunohistochemical localization of betacellulin, a new member of the EGF family, in normal human pancreas and islet tumor cells. *Endocr. J.* **46**, 755–764 (1999).
- Kritzik, M. R. et al. Expression of ErbB receptors during pancreatic islet development and regrowth. *J. Endocrinol.* **165**, 67–77 (2000).
- Huotari, M. A. et al. ErbB signaling regulates lineage determination of developing pancreatic islet cells in embryonic organ culture. *Endocrinology* **143**, 4437–4446 (2002).
- South, J. C., Blackburn, E., Brown, I. R. & Gullick, W. J. The neuregulin system of ligands and their receptors in rat islets of Langerhans. *Endocrinology* **154**, 2385–2392 (2013).
- Guy, P. M., Platko, J. V., Cantley, L. C., Cerione, R. A. & Carraway, K. L. 3rd Insect cell-expressed p180erbB3 possesses an impaired tyrosine kinase activity. *Proc. Natl. Acad. Sci. USA* **91**, 8132–8136 (1994).
- Pinkas-Kramarski, R. et al. ErbB tyrosine kinases and the two neuregulin families constitute a ligand-receptor network. *Mol. Cell Biol.* **18**, 6090–6101 (1998).



35. Elghazi, L., Rachdi, L., Weiss, A. J., Cras-Meneur, C. & Bernal-Miz-rachi, E. Regulation of beta-cell mass and function by the Akt/pro-tein kinase B signalling pathway. *Diab. Obes. Metab.* **9**, 147–157 (2007).
36. Imai, J. et al. Regulation of pancreatic beta cell mass by neuronal signals from the liver. *Science* **322**, 1250–1254 (2008).
37. Leibiger, B. et al. PI3K-C2alpha knockdown results in rerouting of insulin signaling and pancreatic beta cell proliferation. *Cell Rep.* **13**, 15–22 (2015).
38. Yamamoto, J. et al. Neuronal signals regulate obesity induced beta-cell proliferation by FoxM1 dependent mechanism. *Nat. Commun.* **8**, 1930 (2017).
39. Ikushima, Y. M. et al. MEK/ERK Signaling in beta-Cells bifunctionally regulates beta-Cell mass and glucose-stimulated insulin secretion response to maintain glucose homeostasis. *Diabetes* **70**, 1519–1535 (2021).
40. Muller, D., Huang, G. C., Amiel, S., Jones, P. M. & Persaud, S. J. Identification of insulin signaling elements in human beta-cells: autocrine regulation of insulin gene expression. *Diabetes* **55**, 2835–2842 (2006).
41. Folli, F. et al. Altered insulin receptor signalling and beta-cell cycle dynamics in type 2 diabetes mellitus. *PLoS ONE* **6**, e28050 (2011).
42. Gum, R. J. et al. Antisense protein tyrosine phosphatase 1B reverses activation of p38 mitogen-activated protein kinase in liver of ob/ob mice. *Mol. Endocrinol.* **17**, 1131–1143 (2003).
43. Ky, B. et al. Neuregulin-1 beta is associated with disease severity and adverse outcomes in chronic heart failure. *Circulation* **120**, 310–317 (2009).
44. Geisberg, C. A. et al. Circulating neuregulin-1beta levels vary according to the angiographic severity of coronary artery disease and ischemia. *Coron. Artery Dis.* **22**, 577–582 (2011).
45. Wang, R. et al. Decreased plasma levels of neureglin-1 in drug naive patients and chronic patients with schizophrenia. *Neurosci. Lett.* **606**, 220–224 (2015).
46. Yiadom, M. Y. et al. Diagnostic utility of neuregulin for acute cor-onary syndrome. *Dis. Markers* **2016**, 8025271 (2016).
47. Yang, H., Xiao, W., Yang, M., Wang, Y. & Zhang, X. Decreased neuregulin1beta1 in first episode and drug-naive patients with schizophrenia: Negative correlation with cognitive impairment. *Psychiatry Res.* **304**, 114164 (2021).
48. Hamaguchi, M. et al. The severity of ultrasonographic findings in nonalcoholic fatty liver disease reflects the metabolic syndrome and visceral fat accumulation. *Am. J. Gastroenterol.* **102**, 2708–2715 (2007).
49. Siddiqui, M. S. et al. Vibration-controlled transient elastography to assess fibrosis and steatosis in patients with nonalcoholic fatty liver disease. *Clin. Gastroenterol. Hepatol.* **17**, 156–163 (2019).

## Acknowledgements

We are grateful to the members of the Goda lab for technical support and contributions to discussions. We also thank Dr. Elise Lamar for editing the manuscript. This work was supported in part by the MEXT-Supported Program for the Strategic Research Foundation at Private Universities, KAKENHI grants from MEXT/JSPS (17K08674, 20K07345 to N.G.), a Grant-in-Aid for Scientific Research on Innovative Areas “Oxygen Biology: a new criterion for an integrated understanding of life” (No.

2611103 to N.G.), a Waseda University Grant for Special Research Pro-jects (2013B-174, 2014B-313, 2015B-323 to N.G.), and the Takahashi Industrial and Economic Research Foundation (N.G.), and the Japan Research Institute of Industrial Science (N.G.). This work was facilitated by research equipment shared in the MEXT Project for promoting public utilization of advanced research infrastructure (Program for supporting the construction of core facilities, JPMXS0440500023).

## Author contributions

T.A. and N.G. conceived the ideas and contributed to the planning of experiments. T.A., E.H., S.M., A.S., S.W., D.T., Yutaro.O., Yumika.O., M.Y., and Y. S. performed experiments. T.M., H.F., and N.K. contributed to the analysis and interpretation of human data. K.Y. and M.S. contributed to mouse islet preparation and islet experiments. C.Y.K. and M.T. con-tributed to the discussions. N.G. and T.A. wrote and edited the manu-script. All authors approved the final version of the manuscript.

## Competing interests

The authors declare no competing interests.

## Additional information

**Supplementary information** The online version contains supplementary material available at <https://doi.org/10.1038/s41467-025-57167-0>.

**Correspondence** and requests for materials should be addressed to Nobuhito Goda.

**Peer review information** *Nature Communications* thanks the anon-ymous reviewers for their contribution to the peer review of this work. A peer review file is available.

**Reprints and permissions information** is available at <http://www.nature.com/reprints>

**Publisher’s note** Springer Nature remains neutral with regard to jur-isdictional claims in published maps and institutional affiliations.

**Open Access** This article is licensed under a Creative Commons Attribution-NonCommercial-NoDerivatives 4.0 International License, which permits any non-commercial use, sharing, distribution and reproduction in any medium or format, as long as you give appropriate credit to the original author(s) and the source, provide a link to the Creative Commons licence, and indicate if you modified the licensed material. You do not have permission under this licence to share adapted material derived from this article or parts of it. The images or other third party material in this article are included in the article’s Creative Commons licence, unless indicated otherwise in a credit line to the material. If material is not included in the article’s Creative Commons licence and your intended use is not permitted by statutory regulation or exceeds the permitted use, you will need to obtain permission directly from the copyright holder. To view a copy of this licence, visit <http://creativecommons.org/licenses/by-nc-nd/4.0/>.

© The Author(s) 2025